

# Necessary conditions for near edge stick of Complete Contacts

Daniel J. Riddoch<sup>a,\*</sup>, David A. Hills<sup>a</sup>

<sup>a</sup>*Department of Engineering Science, University of Oxford  
Parks Road, Oxford, OX1 3PJ, United Kingdom*

---

## Abstract

The conditions for slip within a contact and at the corner, together with separation conditions are presented in a general sense and applied to two example finite complete contact problems. These conditions can be found directly from the signs of the relevant stress intensity factors. Further, a new bound on the validity of the asymptotic solution is found, and then applied to find a solution relating to separation conditions. Finally this new bound is used to identify and classify cases in which a region of mode *III* dominance is seen from purely geometric considerations.

---

## 1. Introduction

Complete contacts are those in which the front (contacting) faces of the bodies being pressed together have the same shape in the unloaded state, that is they ‘conform’, and the extent of the contact is defined by a discontinuity in the gradient of the profile, as exemplified by the rectangular block-on-half plane arrangement shown in Figure 1. They have the property that the contact size is independent of the load carried and that a stress singularity will usually arise at the edges of the contact. Practically occurring contacts which are of this general form include splines, for example in certain car transmissions and in the split shafts of a gas turbine.

The object of the analysis presented here is to quantify the conditions for ensuring that the contact edges are stuck so that fretting damage is avoided, although this does leave the attendant risk of a notch type failure. We shall assume that the block and the half-plane are made from the same material, and also that the interface is, indeed, straight, as sketched, but note that the results to be found would apply equally well to a circular cylinder resting in a conforming groove, provided that the line of the interface were accounted for correctly.

A full analysis of the problem, including incorporating the presence of all features, calls for a finite element analysis and, indeed, finite element analysis must be used to calibrate the external loads to stress intensity factors to be defined, but our object is to learn as much as possible about the properties of the contact from an analysis of the half-plane and contact corner modelled together, as a monolith, and using Williams’ analysis of a wedge [1] as our starting point. The use of this classic asymptotic form, appropriate when the observation point is much nearer to the corner than any other features, adds considerable precision to our understanding of the local stress field.

This idea is one which we have used before. It enables the coefficient of friction needed to attain a fully stuck contact edge [2] to be determined. But in that analysis only the dominant term in an eigenfunction expansion was used, and the question arises of what happens when we move slightly inwards from the edge; is the coefficient of friction needed to achieve stick at the

---

\*Corresponding Author

Email address: [daniel.riddoch@eng.ox.ac.uk](mailto:daniel.riddoch@eng.ox.ac.uk) (Daniel J. Riddoch)

edge also sufficient to attain stick in the rest of the neighbourhood? We answer that question, here, together with looking at further forms of excitation of the local stress field.

One of the main topics of practical analysis in this laboratory is the study of fretting, and fretting fatigue, and in pursuing these we note that there are normally four sets of external loads which are relevant in describing the local contact-edge stress field, (Figure 1), viz. the normal load,  $P$ , the shear force,  $Q$ , any moment carried by the contact-defining body,  $M$ , and underlying surface tension in the counterbody,  $\Delta\sigma$ . All of these quantities become ‘coupled’ in the context of a complete contact, in the sense that all four excite all eigenmodes. Here, we will concentrate on only the first two terms in the infinite Williams series, and investigate what these imply. This is a legitimate approximation to make as these are the only two terms in the series which are singular at the contact edge, all others terms being bounded. Hence, these terms dominate the solution.

## 2. Formulation

It is initially assumed that the two contacting bodies are in intimate contact everywhere, and fully adhered, giving a monolithic domain. We zoom in on the contact (wedge) corner. At the time of the initial consideration of this class of problem, we would write down the state of stress in the neighbourhood of the wedge (contact) corner [1] in the form

$$\sigma_{ij}(r, \theta) = K_I r^{\lambda_I - 1} f_{ij}^I(\theta) + K_{II} r^{\lambda_{II} - 1} f_{ij}^{II}(\theta) + \dots \quad (1)$$

where  $(r, \theta)$  are polar coordinates measured from the notch bisector, Figure 1,  $(K_I, K_{II})$  are the multipliers (generalised stress intensity factors) which match the eigensolution to the finite problem,  $f_{ij}^K(\theta)$  are the eigenvectors (see Appendix A), and the eigenvalues  $(\lambda_I, \lambda_{II})$  are given by the smallest, positive, non-trivial root of the following characteristic equations

$$\lambda_I \sin(2\alpha) + \sin(2\alpha\lambda_I) = 0 \quad \& \quad \lambda_{II} \sin(2\alpha) - \sin(2\alpha\lambda_{II}) = 0 \quad (2)$$

where  $2\alpha$  is the total wedge angle, and equal to  $\pi + \phi$ , where  $\phi$  is the internal angle of the block, equal to  $\pi/2$  in Figure 1 but to be generalised later. The angles are measured from the bisector as the eigensolutions uncouple along that line, and we also use this angular position to define the values of the generalised stress intensity factors, ie.

$$K_I = \lim_{r \rightarrow 0} \sigma_{\theta\theta}(r, 0) r^{1-\lambda_I} \quad f_{r\theta}^I(r, 0) = 0 \quad \& \quad f_{\theta\theta}^I(r, 0) = 1 \quad (3)$$

and

$$K_{II} = \lim_{r \rightarrow 0} \sigma_{r\theta}(r, 0) r^{1-\lambda_{II}} \quad f_{\theta\theta}^{II}(r, 0) = 0 \quad \& \quad f_{r\theta}^{II}(r, 0) = 1 \quad (4)$$

Before introducing an alternative representation of this solution, we will consider the physical requirements for the solution to be developed to be appropriate when applied to contact problems. These are; (a) that the two bodies be in intimate contact, implied by  $\sigma_{\theta\theta}(r, \psi) < 0$ , where  $\psi = \frac{1}{2}(\pi - \phi)$  is the angle to the interface, and (b) stick must prevail which requires  $-|\sigma_{r\theta}(r, \psi)| / \sigma_{\theta\theta}(r, \psi) < f$ , where  $f$  is the coefficient of friction, for all points ‘ $r'$ ’ on the interface. Some *local* violations of these inequalities may be tolerated without invalidating the whole solution, but first consider conditions where they *are* satisfied everywhere.

For the time being, focus attention wholly on the square block, Figure 1, so that  $2\alpha = 3\pi/2$  and  $\psi = \pi/4$ . For this example the eigenvectors  $(f_{ij}^I(\theta), f_{ij}^{II}(\theta))$  are given in Appendix A. We note that  $f_{\theta\theta}^I(\pi/4) \simeq 0.7$  so that it follows, because we can always find points sufficiently close to the contact corner for the mode I contribution to dominate the solution, a requirement for

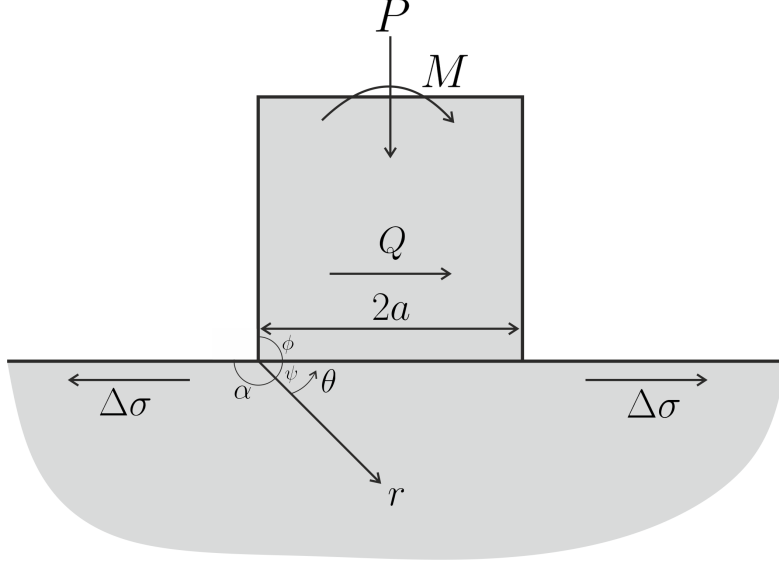


Figure 1: Rectangular block resting on a half-plane subject to four external loads

the contact edge to remain closed is that  $K_I < 0$ . If we turn our attention, now, to the second term in the series, it has been shown in the appendix that  $f_{\theta\theta}^{II}(\pi/4) \simeq -1.2$  so that if  $K_{II} > 0$  we could be confident that the penetration of intimate contact inwards from the contact edge will last to at least the point where the contributions to the overall solution from modes  $I$  and  $II$  loading were equal. The question arises ‘Physically, where is the point along the interface where mode I domination of the solution gives way to a contribution from the second solution which is of at least comparable magnitude?’ and to answer we may re-write the first two terms of equation (1), which brings out the internal length scale,  $d_0$ , and introduce this quantity and a further quantity,  $G_0$ , which has dimensions of stress, defined by [3],

$$d_0 = \left| \frac{K_{II}}{K_I} \right|^{\frac{1}{\lambda_I - \lambda_{II}}} \quad (5)$$

$$G_0 = |K_I|^{\frac{\lambda_{II}-1}{\lambda_{II}-\lambda_I}} |K_{II}|^{\frac{\lambda_I-1}{\lambda_{II}-\lambda_I}}, \quad (6)$$

so that equation (1) may be re-written as

$$\frac{\sigma_{ij}(r, \theta)}{G_0} = \left( \frac{r}{d_0} \right)^{\lambda_I-1} f_{ij}^I(\theta) - \left( \frac{r}{d_0} \right)^{\lambda_{II}-1} f_{ij}^{II}(\theta). \quad (7)$$

This form is extremely useful for studying notch-corner plasticity [3], and highlights that  $d_0$  may be viewed as the notional radial distance which represents the partition between mode  $I$  domination ( $r < d_0$ ) and higher order terms domination ( $r > d_0$ ). It may also be used in our present study: although it is not possible to state unequivocally the distance from the contact corner where higher order terms in a series representation dominate the solution, it is possible to define the distance where the mode I term loses its significance, viz.  $d_0$ . This quantity is defined wholly by the mode mixity (equation (5)), and in cases where this exceeds the distance to the nearest physically relevant feature (for example the contact half width, Figure 1), then we can

be assured that the first term controls the state of stress until the observation point reaches this feature dominates.

### 3. A remark on separation

It is well known that we may always find a point, sufficiently close to the corner, where the stress state is totally dominated by the mode  $I$  term. It's sign is determined by the sign of the stress intensity factor  $K_I$ . Hence the lift-off or intimate contact of the corner itself is determined by the sign of this term alone, which is both loading and geometry dependent.

We now suppose that the edge of the contact is intimately closed but consider the possibility of lift-off at a point *within* the body, according to the asymptotic results. For this to occur, and to be observable within the asymptote, we require a turning point in the equation

$$\sigma_{\theta\theta} = K_I f_{\theta\theta}^I r^{\lambda_I-1} + K_{II} f_{\theta\theta}^{II} r^{\lambda_{II}-1}, \quad (8)$$

found by  $\frac{d\sigma_{\theta\theta}}{dr} = 0$ . This is shown in Figure 2, where in the central sketch we see a case where such a turning point exists, and how this may lead to an internal lift-off point.

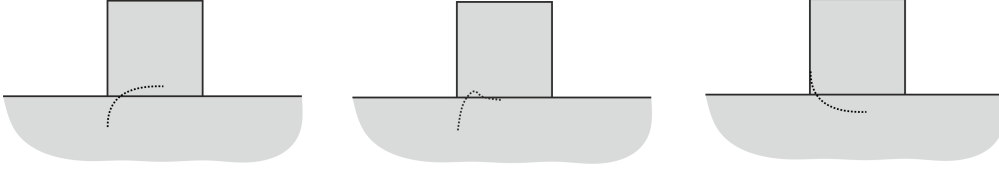


Figure 2: Sketch of different possible shapes for  $\sigma_{\theta\theta}$

The location of this point is given by

$$r = \frac{-K_I}{K_{II}}^{\frac{\lambda_I-2}{\lambda_{II}-2}} \left( \frac{f_{\theta\theta}^I(\lambda_I-1)}{f_{\theta\theta}^{II}(\lambda_{II}-1)} \right)^{\frac{\lambda_I-2}{\lambda_{II}-2}}. \quad (9)$$

Note that the quantity within brackets depends only on  $\alpha$ , so the behaviour of the function is governed by the ratio  $K_I/K_{II}$ . Therefore for a given geometry, the behaviour and/or existence of such a turning point is purely loading dependent.

#### 3.1. Application to the 90° block

Retaining a focus on the square block resting on a halfplane, we aim to improve on and refine the conditions set out by Churchman[4] for separation at the edge of the contact and within the body, as far as is possible with only asymptotic considerations.

To do this, we use a finite element analysis of the problem to calibrate the external loading with the stress intensity factors. This is done by modelling the problems then applying each of the four external loads individually. The stresses along the angle bisector are then found from FE, and the limits taken as described above in equations (3) and (4). The results of this for the square block are shown in equation 10. However, we will first concentrate on excitation by only

a normal force  $P$  and a shear force applied along the line of the interface,  $Q$ .

$$\begin{bmatrix} K_I a^{\lambda_I-1} \\ K_{II} a^{\lambda_{II}-1} \end{bmatrix} = \begin{bmatrix} -0.2265 & 0.2443 & -0.3890 & 0.2462 \\ 0.1118 & 0.2536 & 0.3639 & 0.1483 \end{bmatrix} \begin{bmatrix} \frac{P}{2a} \\ \frac{Q}{2a} \\ \frac{M}{2a^2} \\ \frac{\Delta\sigma}{2} \end{bmatrix} \quad (10)$$

From the calibration, we see that the value of  $Q/P$  required to cause lift off at the corner is  $Q/P = 0.927$ . This differs slightly from the value found by Churchman[4], but this is purely due to differences in the calibrations from finite element analysis. The details of this analysis are discussed in AppendixB.

We now intend to see how the location of the turning point (equation (9)) changes with changes in normal and shear load. We can see from Figure 3(a) the ratio  $K_I/K_{II}$  is negative for values of  $Q/P$  is in the range  $-0.44 < Q/P < 0.927$ . This implies an *internal* lift off point cannot be found once the loading ratio is within the range needed to maintain intimate contact at the corner, as the location of this turning point, as given by equation (9) is negative and hence outside the contact patch.

The positive value of the ratio  $K_I/K_{II}$  for negative values of  $Q/P$  would appear to imply that the corner would lift-off too for values of  $Q/P < -0.44$ . However, looking at Figure 3(b) we see that for values, roughly,  $Q/P < 0.2$ , the ratio  $d_0/a > 1$ , ie. the mode *II* term dominates the mode *I* term only at a point beyond the centre of the contact, beyond where the asymptotic solution can be assumed to apply. Therefore all points along the interface are mode *I* dominated, so the stress may be described by  $\sigma_{\theta\theta} = K_I f_{\theta\theta}^I r^{\lambda_I-1}$  alone, which displays no turning point, and hence intimate contact is maintained within the asymptote for this load region as  $K_I < 0$ , giving  $\sigma_{\theta\theta} < 0$  which is compressive.

So, for the 90° block, at least, we cannot improve on the statement presented by Churchman by the use of a two-term solution. We conclude that lift-off only occurs in the near edge when  $K_I$  is positive. Further inferences on the effect of other methods of loading are made in section 4.2.1, together with observations on their effect on slip conditions.

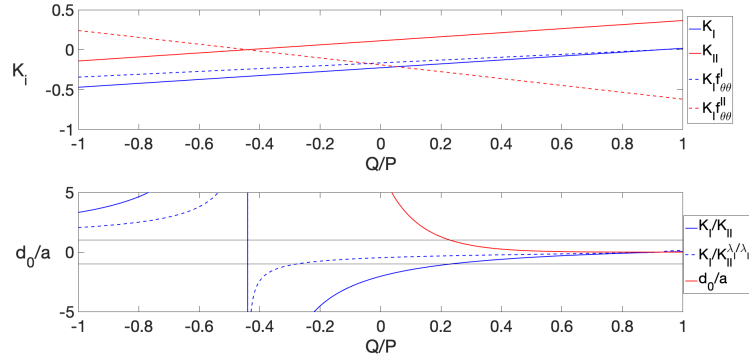


Figure 3: The variation of stress intensity factors and resultant constants with varying  $Q/P$

#### 4. Slip

As laid out at the start of this paper, one of the objects of this analysis is to determine the conditions required for the corners of the contact to remain stuck, in order to avoid fretting

damage. Equally important is ensuring that there is no region of slip *within* the body, which would equally lead to fretting damage.

Recall from Hills and Dini [3] that the corner will slip for a sufficiently low coefficient of friction. Hence, we must determine under what conditions slip will occur within the body, and within the asymptote, or at the corner. As already discussed in section 3, there are conditions under which we get lift-off at the corners of the block. This will necessarily lead to some partial slip. We deduce this because the direct traction( $\sigma_{\theta\theta}$ ) changes sign, so must fall smoothly to zero in the region just interior to the true point of separation. Recall, further, that it was noted that a shear force had to be present to induce separation. The shear traction( $\sigma_{r\theta}$ ) will be non-zero local to the point of separation. So, there must exist a point where the equation  $\sigma_{r\theta} = f\sigma_{\theta\theta}$  is satisfied. Hence, this point will be slipping.

#### 4.1. The turning point

To determine whether an interior point is the point of first slip, let us first consider the ratio  $\sigma_{r\theta}/\sigma_{\theta\theta}$ . If this ratio is greater than the coefficient of friction over some distance, slip will occur there; if not, it will remain stuck. So, we will find the turning point of this ratio, as either the value near to this point, or the contact edge value, will give the coefficient of friction required to prevent all slip.

The turning point can be found by

$$\frac{d}{dr} \left( \frac{\sigma_{r\theta}}{\sigma_{\theta\theta}} \right) = - \frac{(f_{r\theta}^{II} f_{\theta\theta}^I - f_{r\theta}^I f_{\theta\theta}^{II})(\lambda_I - \lambda_{II}) r^{\lambda_I + \lambda_{II} - 1} K_I K_{II}}{(f_{\theta\theta}^I K_I r^{\lambda_I} + f_{\theta\theta}^{II} K_{II} r^{\lambda_{II}})^2} = 0. \quad (11)$$

Provided that the denominator is non-zero, we may first deduce that we can in fact solve the equation

$$-(f_{r\theta}^{II} f_{\theta\theta}^I - f_{r\theta}^I f_{\theta\theta}^{II})(\lambda_I - \lambda_{II}) r^{\lambda_I + \lambda_{II} - 1} K_I K_{II} = 0. \quad (12)$$

Now set

$$A = f_{r\theta}^{II} f_{\theta\theta}^I - f_{r\theta}^I f_{\theta\theta}^{II} \quad B = -(\lambda_I - \lambda_{II}) \quad C = r^{\lambda_I + \lambda_{II} - 1} K_I K_{II} \quad (13)$$

So equation (12) becomes

$$ABCK_I K_{II} = 0.$$

From Williams solution we have that  $\lambda_{II} > \lambda_I$  so we find that  $B > 0$ . Secondly, we consider positive  $r$  only, ie within the block, so  $C > 0$ . Finally we cannot easily see algebraically, but on plotting  $A$  we find that  $A > 0$ . Hence we have that the solutions to equation 11 are given by  $K_I = 0$  or  $K_{II} = 0$ .

So a turning point can exist only if  $K_I = 0$  or  $K_{II} = 0$ . In these cases the ratio  $\sigma_{r\theta}/\sigma_{\theta\theta}$  is equal to  $f_{r\theta}^{II}/f_{\theta\theta}^{II}$  and  $f_{r\theta}^I/f_{\theta\theta}^I$  respectively, and is independent of  $r$ . Hence, all we can say is that in the first case( $K_I = 0$ ) we will always see slip at the corner, and in the second, we will see slip at the corner if  $f < f_{r\theta}^I/f_{\theta\theta}^I$ , provided that  $K_I < 0$ . The independence of these ratios from  $r$  means that we cannot say what happens at any point other than the corner.

For all other cases,  $K_I \neq 0$  and  $K_{II} \neq 0$ , we can say that there is no turning point within the asymptote, so, either slip will start at the corner, or within the body but beyond the asymptote. We can determine which of these cases applies by looking at the gradient of the ratio  $\sigma_{r\theta}/\sigma_{\theta\theta}$ . This could be found by taking the limit of the expression in equation 11 as  $r \rightarrow 0$ , but this limit does not exist. So instead, we find the sign of the expression in the same way the conditions for the existence of a turning point were found.

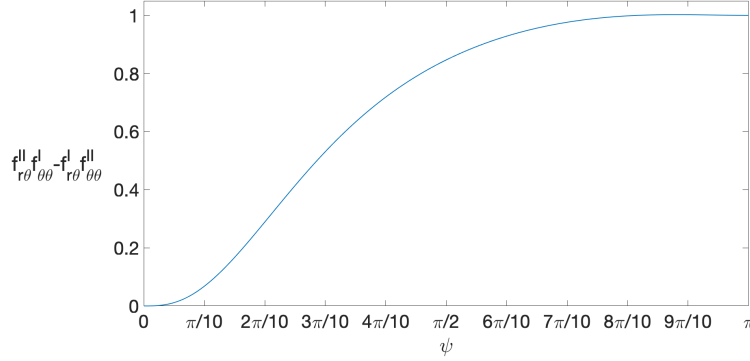


Figure 4: Value of  $f_{r\theta}^{II} f_{\theta\theta}^I - f_{r\theta}^I f_{\theta\theta}^{II}$  with  $\psi$

		$K_I$	
	Sign of $K_i$	Positive	Negative
$K_{II}$	Positive	Separation and entire asymptote slip(A)	Slip starts at corner(B)
	Negative	Separation and small slip region(C)	Slip from within(D)

Table 1: Matrix of inferred result from stress intensity factor signs

Recall that

$$\text{sign}(-(f_{r\theta}^{II} f_{\theta\theta}^I - f_{r\theta}^I f_{\theta\theta}^{II})(\lambda_I - \lambda_{II})r^{\lambda_I + \lambda_{II} - 1} K_I K_{II}) = \text{sign}(K_I K_{II}) \quad \text{and} \quad (14)$$

$$\text{sign}((f_{\theta\theta}^I K_I r^{\lambda_I} + f_{\theta\theta}^{II} K_{II} r^{\lambda_{II}})^2) \neq -1. \quad (15)$$

Hence,

$$\text{sign}\left(\frac{d}{dr} \frac{\sigma_{r\theta}}{\sigma_{\theta\theta}}\right) = \text{sign}(K_I K_{II}),$$

whenever the gradient is determinable.

The results here are interesting. We know that if  $d(\sigma_{r\theta}/\sigma_{\theta\theta})/dr$  is positive, then slip will begin within the body, at some point beyond the validity of the asymptote. However, in the case where  $K_I$  is positive, the corner will also be slipping, giving a large region of slip. Whereas, if  $K_I$  is negative, slip will originate at a point within the body with  $f > f_{r\theta}^I/f_{\theta\theta}^I$ , but for some coefficients of friction, given by Hills and Dini [3], stick will persist at the corner. The reverse is true if the gradient is negative, and slip will always originate at the corner provided  $K_I < 0$ , for  $f < f_{r\theta}^I/f_{\theta\theta}^I$ . If  $K_I$  is positive, then, as already outlined, slip will start at the corner but stick will persist within the body and, for sufficiently large coefficients of friction, within the asymptote. These results are summarised in Table 1.

#### 4.2. Application to the 90° block

Returning focus to the 90° block, we may distinguish the regions of the load space where each of these forms of behaviour occurs. The results of this analysis are shown in Figure 5. The letters shown correspond to those defined in table 1. Note that, under these loading conditions, there is no region in which  $K_I > 0$  and  $K_{II} < 0$ .

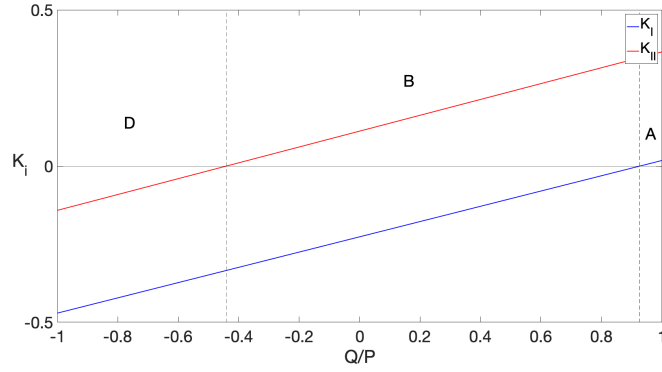


Figure 5: Plot showing the regions of behaviour for the 90 degree block

#### 4.2.1. Further forms of loading

So far we have considered excitation only by a normal and shearing force, and we have assumed that these are not sufficient to cause sliding, ie.  $|Q|/fP < 1$ . However, excitation by other means is possible and the appropriate calibrations for the  $90^\circ$  block were included in equation (10).

We can divide the load space to characterise behaviour under general loading as we did with just two loading types. Figure 6 shows the results of these where, in each, one of loading methods is not excited. Consequently we can see the load regions where each of these types of behaviour occur, again the letters refer to those in Table 1.

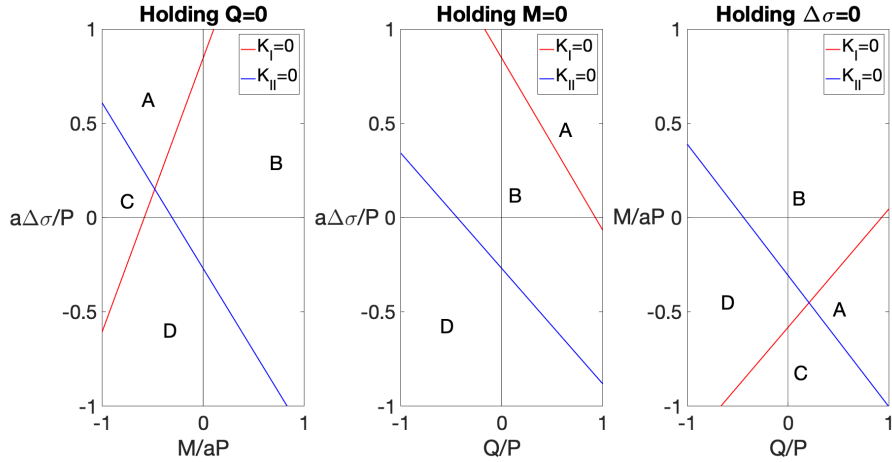


Figure 6: Characterisation of regions of the four method load space(see Table 1)

## 5. A further bound on asymptotic validity

From section 3, we can see that, provided that the corner is in intimate contact, the whole interface, within the region which can be approximated by the asymptotic solution, must remain in intimate contact. In other words, throughout the region of asymptotic validity,  $\sigma_{\theta\theta} < 0$ ,



provided that conditions are such that the corner itself is in intimate contact. A tidier way to locate the point where the interfacial direct traction changes sign is to find a solution to  $\sigma_{\theta\theta} = 0$ . This point is itself beyond the limit of the validity of the asymptotic solution, but can provide an upper bound.

So, we solve the equation evaluated on  $\theta = \psi$

$$K_I f_{\theta\theta}^I(\psi) r^{\lambda_I-1} + K_{II} f_{\theta\theta}^{II}(\psi) r^{\lambda_{II}-1} = 0 \quad (16)$$

to find the value of  $r$  which satisfies this. We denote this value by  $d_r$ , its value is given by

$$d_r = \left( \frac{-f_{\theta\theta}^{II}(\psi)}{f_{\theta\theta}^I(\psi)} \right)^{\frac{1}{\lambda_I - \lambda_{II}}} \left( \frac{K_{II}}{K_I} \right)^{\frac{1}{\lambda_I - \lambda_{II}}}. \quad (17)$$

So we can state, using this bound, that for the stresses at a point,  $s$  along the interface to be approximated by the asymptotic solution, it is a necessary but not sufficient condition that  $s/d_r < 1$ .

## 6. Consideration of other angles

So far, throughout this paper our examples have been limited to a square block resting on half plane, however it is not necessary to do this and the general results presented are equally applicable to any complete contact. An obvious extension is to take the internal angle of the block as a parameter,  $\psi$ . In order to apply these results to a new example, it is necessary to perform calibrations by finite element analysis to find the stress intensity factors. Otherwise, however, we may proceed as for the 90 degree block. The details of this analysis are discussed in AppendixB. Several such calibrations have been done and included here is such a calibration, whose internal angle is  $\arctan(-3/4) \approx 143^\circ$ . This is chosen so as to display a mode  $II$  dominant region, as explained in section 7.

$$\begin{bmatrix} K_I a^{\lambda_I-1} \\ K_{II} a^{\lambda_{II}-1} \end{bmatrix} = \begin{bmatrix} -0.2260 & 0.1070 & -0.4415 & 0.1516 \\ 0.0369 & 0.2711 & 0.0930 & 0.1094 \end{bmatrix} \begin{bmatrix} \frac{P}{2a} \\ \frac{Q}{2a} \\ \frac{M}{2a^2} \\ \frac{\Delta\sigma}{2} \end{bmatrix} \quad (18)$$

Use of this calibration leads us to conclude that under no combination of pure  $P, Q$  loading does this block lift-off at the corner, see Figure 8, but it can be made to do so by using other methods of loading, as in Figure 9, however, only for large values of the ratios  $a\Delta\sigma/P$  and  $M/aP$ . The argument against an interior lift-off point that applied to the  $90^\circ$  block applies again here, as can be seen in Figure 7.

Slip consideration can also be made, and the letters shown in figures 8 and 9 relate again to table 1, which is still applicable here. Common throughout all of these, is that, for moderate loading, and largely for positive valued loading(as defined by convention in Figure 1), slip will originate from the corner, regions marked ‘B’, and hence the conditions necessary to prevent slip at the corner are sufficient to prevent interfacial slip throughout the interface.

## 7. A bound on the existence of mode $II$ dominated regions

Throughout this analysis we have utilised a two-term analysis. We have already seen that it is always possible to find a point where the state of stress is dominated by the first term in our

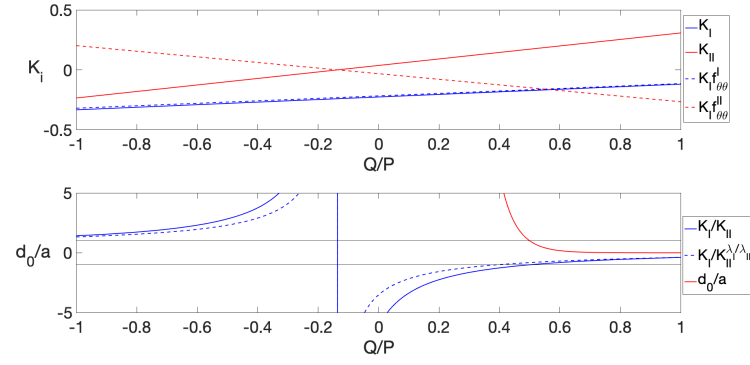


Figure 7: The variation of stress intensity factors and resultant constants with varying  $Q/P$  for the  $143^\circ$  block

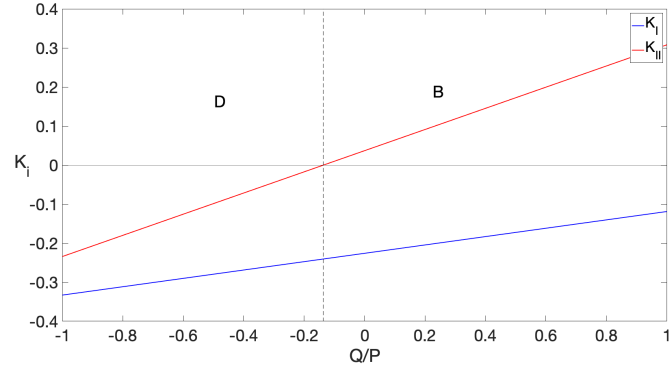


Figure 8: Plot showing the regions of behaviour for the  $143^\circ$  block

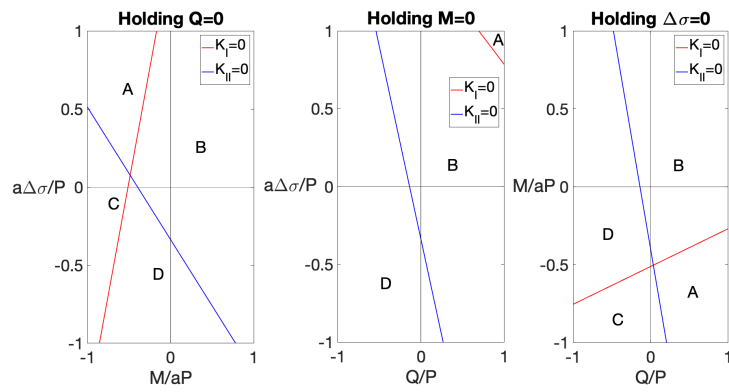


Figure 9: Characterisation of slip behaviours of the  $143^\circ$  block in four load space

expansion. However, we now ask whether the same can be said for the second term. We already know that these points, should they exist, would be at a point  $r > d_0$ . We also know that for them to be valid for consideration with asymptotic methods, we require  $r < d_r$ . So it is natural to conclude that we require the ratio  $d_r/d_0 > 1$ , for asymptotic consideration to be appropriate. A comparison of the forms of these values leads to the ratio

$$\frac{d_r}{d_0} = \left( \frac{-f_{\theta\theta}^{II}(\psi)}{f_{\theta\theta}^I(\psi)} \right)^{\frac{1}{\lambda_I - \lambda_{II}}} . \quad (19)$$

Plotting this we find that, as shown in Figure 10, the value  $d_r/d_0 = 1$  is achieved at approximately  $\alpha = \alpha_0 = 0.89\pi$ , or alternatively  $\psi = \psi_0 = 139^\circ$ . Consequently, we cannot find a point where the mode  $II$  term dominates the mode  $I$  and which is within the valid range of the asymptote, for values of  $\alpha < 0.89\pi$ . So we cannot see a region of mode  $II$  dominance for an indenter of internal angle less than  $139^\circ$ .

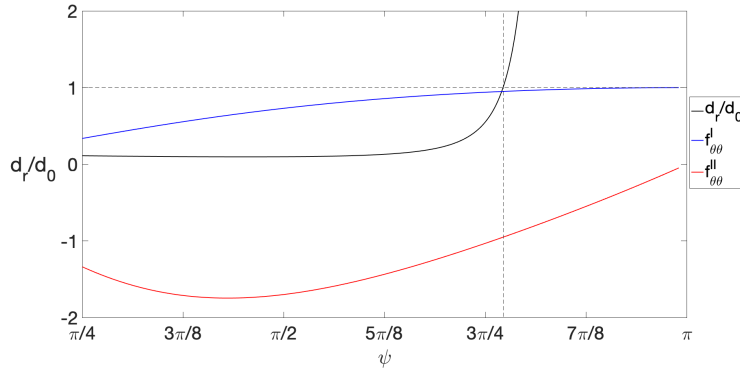


Figure 10: The value of the ratio  $d_r/d_0$  with varying total internal angle  $\alpha$

### 7.1. A new normalised form of the solution

Finally, we may use  $d_r$  to re-write the equation for  $\sigma_{ij}$  in a different way.

$$\frac{\sigma_{ij}(r, \psi)}{G_r} = \left( \frac{r}{d_r} \right)^{\lambda_I - 1} - \left( \frac{r}{d_r} \right)^{\lambda_{II} - 1} \quad (20)$$

where

$$G_r = \left( \frac{K_I}{f_{ij}^I(\psi)} \right)^{\frac{\lambda_{II} - 1}{\lambda_I - \lambda_{II}}} \left( -K_{II} f_{ij}^{II}(\psi) \right)^{\frac{\lambda_I - 1}{\lambda_I - \lambda_{II}}} \quad (21)$$

$$d_r = \left( \frac{-f_{ij}^{II}(\psi)}{f_{ij}^I(\psi)} \right)^{\frac{1}{\lambda_I - \lambda_{II}}} \left( \frac{K_{II}}{K_I} \right)^{\frac{1}{\lambda_I - \lambda_{II}}} \quad (22)$$

## 8. Conclusions

The object of this analysis was to gain extra information about the form of the solution from a two-term asymptotic consideration, compared to that found using a single-term approximation. This has proven to be a difficult task. However, several general conclusions can be drawn from the work presented.

A set of conditions which categorise slip behaviour solely from the signs of the relevant stress intensity factors has been devised. We find that, in cases with positive  $K_{II}$ , the coefficient of friction required to prevent slip at the corner is sufficient to prevent any slip within the asymptote. The same is not true when  $K_I$  is negative, with slip starting within the body. This allows, with appropriate finite element calibrations, for the categorisation of four load space into four regions of distinct behaviour covering the entire space.

Further, a bound on the validity of asymptotic solutions was established and from this, a new normalisation of the Williams solution is possible. Also resulting is a bound on indenter angle necessary for a mode  $II$  dominant region to be visible by asymptotic methods is established.

## 9. Acknowledgements

Both authors thank Rolls-Royce plc and the EPSRC for the support under the Prosperity Partnership Grant 'Cornerstone: Mechanical Engineering Science to Enable Aero Propulsion Futures', Grant Ref: EP/R004951/1.

## 10. References

- [1] M. Williams, Stress singularities resulting from various boundary conditions in angular corners of plates in extension, *Journal of applied mechanics* 19 (4) (1952) 526–528.
- [2] D. Hills, D. Dini, What level of friction guarantees adhesion in a complete contact?, *The Journal of Strain Analysis for Engineering Design* 39 (5) (2004) 549–551.
- [3] D. A. Hills, D. Dini, Characteristics of the process zone at sharp notch roots, *International Journal of Solids and structures* 48 (14-15) (2011) 2177–2183.
- [4] C. M. Churchman, D. A. Hills, General results for complete contacts subject to oscillatory shear, *Journal of the Mechanics and Physics of Solids* 54 (6) (2006) 1186–1205.
- [5] J. R. Barber, *Elasticity*, Springer, 2010.

## Appendix A. Williams solution

A full description and derivation of the Williams solution can be found either from the original [1] or from Elasticity [5]. However, a simple outline of certain important points is given here. Firstly, we consider the eigenvalues, which are found as the solutions to the characteristic equations

$$\lambda_I \sin(2\alpha) + \sin(2\alpha\lambda_I) = 0 \quad \& \quad \lambda_{II} \sin(2\alpha) - \sin(2\alpha\lambda_{II}) = 0. \quad (\text{A.1})$$

We note that we have certain conditions placed on these solutions  $\lambda_I$  and  $\lambda_{II}$ . We require that both be positive, and that  $\lambda_{II} > \lambda_I$ , except in the special case  $\psi = \pi$ , in which case we find  $\lambda_I = \lambda_{II} = 0.5$ . Further more we require  $\lambda_I \neq 1$  and  $\lambda_{II} \neq 1$  as these would lead to trivial solutions.

The eigenvectors of the solution are given by the equations

$$f_{rr}^I(\psi) = \frac{\cos[(\lambda_I - 1)\alpha] \cos[(\lambda_I + 1)\psi] - \frac{\lambda_I - 3}{\lambda_I + 1} \cos[(\lambda_I + 1)\alpha] \cos[(\lambda_I - 1)\psi]}{\cos[(\lambda_I + 1)\alpha] - \cos[(\lambda_I - 1)\alpha]} \quad (\text{A.2})$$

$$f_{rr}^{II}(\psi) = \frac{\sin[(\lambda_{II} - 1)\alpha] \sin[(\lambda_{II} + 1)\psi] - \frac{\lambda_{II} - 3}{\lambda_{II} + 1} \sin[(\lambda_{II} + 1)\alpha] \sin[(\lambda_{II} - 1)\psi]}{\sin[(\lambda_{II} - 1)\alpha] - \frac{\lambda_{II} - 1}{\lambda_{II} + 1} \sin[(\lambda_{II} + 1)\alpha]} \quad (\text{A.3})$$

$$f_{r\theta}^I(\psi) = \frac{\sin[(\lambda_I - 1)\alpha] \sin[(\lambda_I + 1)\psi] - \sin[(\lambda_I + 1)\alpha] \sin[(\lambda_I - 1)\psi]}{\sin[(\lambda_I - 1)\alpha] - \frac{\lambda_I - 1}{\lambda_I + 1} \sin[(\lambda_I + 1)\alpha]} \quad (\text{A.4})$$

$$f_{r\theta}^{II}(\psi) = \frac{\cos[(\lambda_{II} - 1)\alpha] \cos[(\lambda_{II} + 1)\psi] - \cos[(\lambda_{II} + 1)\alpha] \cos[(\lambda_{II} - 1)\psi]}{\cos[(\lambda_{II} - 1)\alpha] - \cos[(\lambda_{II} + 1)\alpha]} \quad (\text{A.5})$$

$$f_{\theta\theta}^I(\psi) = \frac{\cos[(\lambda_I - 1)\alpha] \cos[(\lambda_I + 1)\psi] - \cos[(\lambda_I + 1)\alpha] \cos[(\lambda_I - 1)\psi]}{\cos[(\lambda_I - 1)\alpha] - \cos[(\lambda_I + 1)\alpha]} \quad (\text{A.6})$$

$$f_{\theta\theta}^{II}(\psi) = \frac{\sin[(\lambda_{II} - 1)\alpha] \sin[(\lambda_{II} + 1)\psi] - \sin[(\lambda_{II} + 1)\alpha] \sin[(\lambda_{II} - 1)\psi]}{-\sin[(\lambda_{II} - 1)\alpha] + \frac{\lambda_{II} - 1}{\lambda_{II} + 1} \sin[(\lambda_{II} + 1)\alpha]} \quad (\text{A.7})$$

## Appendix B. Finite element modelling

Mentioned throughout this paper is the finite element calibration used in examples. We now briefly discuss how this modelling was done, some of the precautions taken to ensure an accurate and reliable calibration. The modelling technique was the same for both examples, but here we discuss the 90° block. All of the modelling was done using the commercial FE code ABAQUS.

In this case, we have a square block, of side length  $2a$  resting on a half-plane. We assumed intimate contact so we may model this system as a single monolith. The halfplane was represented by a square block of side length  $100a$ . The combined shape of the half-plane and the smaller block make up the monolith. This means that no assumptions need to be made about the contact, such as coefficient of friction.

A mesh of standard linear plane strain elements was used, with 100 elements along the bisector. This mesh was settled on after mesh dependency analysis was performed and this found to be sufficient to capture the effects of the singularity.

The half-plane was then constrained on its bottom edge to with a pinned boundary condition. A uniform distribution of pressure on the top face served to apply the normal force. A concentrated shear force was applied to the top of the block, with a corresponding moment to cancel the moment created by this, being equivalent to applying the load along the interface. This moment, and the moment applied directly were applied by a two forces at the corners of the block, acting as a couple. Finally a negative pressure was applied to the half-plane to act as the bulk tension.

In this last case, the boundary conditions were changed to restrict a single central point on the bottom of the half-plane, not the entire surface.